Bull. Mater. Sci., Vol. 17, No. 2, April 1994, pp. 153–162. © Printed in India.

Flux dynamics of YBCO/Ag composite

INDU DHINGRA, B K DAS and S C KASHYAP*
Materials Division, National Physical Laboratory, New Delhi 110012, India
*Centre for Materials Science and Technology, Indian Institute of Technology, New Delhi 110016, India

MS received 29 October 1993; revised 10 January 1994

Abstract. DC magnetization measurements have been carried out on bulk YBCO/Ag composites with silver content up to 20 wt per cent. DC fields in the range 0·5 mT to 200 mT have been used to investigate the inter- and intragranular properties at 77 K. The AC susceptibility as a function of temperature at different AC fields (0·026–0·30 mT) has also been studied. Under small DC fields (≈ 4 mT), depending on the Ag content and H_{max}, the M–H loop shows a complicated behaviour. This behaviour can be explained on the basis of effect of strong field dependence of transport critical current, grain size and intragrain critical current density J_{cgm} on low-field M–H loop. The estimation of intergranular critical current density J_{cjm} from these loops does not remain a simple function of $\Delta M/d$. The AC susceptibility measurements show a small increase in $J_c(T)$ with silver content under low AC fields only, consistent with the transport J_c data; beyond that $J_c(T)$ decreases. This improvement in $J_c(T)$ and transport J_c with silver can be ascribed to the improved coupling between grains but not to the pinning. Also at higher field ($H_{max} > 20$ mT) the addition of Ag decreases the intragrain critical current density. The upper critical field of intergranular region H_{c2j} and lower critical field of intragrain region H_{c1g} also decrease with silver content.

Keywords. Flux dynamics; YBCO/Ag composite.

1. Introduction

Studies of silver addition to high-temperature superconductors have been motivated by the hypothesis that the intergrain resistance which limits the high critical currents (J_c) could be reduced by the presence of silver in the intergranular region of the sample. Addition of silver in YBCO offers many advantages and some apparent disadvantages. The silver resides mainly at the grain boundaries (Saito *et al* 1987; Pavuna *et al* 1988) where it inhibits corrosion and does not influence critical temperature, T_c (Matsumoto *et al* 1990). It essentially forms a YBCO/Ag composite. It was reported that addition of silver reduces the normal state resistivity (Dwir *et al* 1989; Sen *et al* 1989) and enhances the transport critical current density in YBCO (up to 30 wt% of Ag) by a factor of 2–3, measured at 77 K under zero applied magnetic field (Jung *et al* 1990; Dhingra *et al* 1991). The mechanical properties also improved with the addition of silver (Singh *et al* 1989; Ren *et al* 1990). Silver causes significant grain growth with better intergranular connectivity through partial melting of YBCO (Tiefel *et al* 1988; Baliga and Jain 1989).

The improvement in the transport critical current density of YBCO/Ag composites can be attributed either to improved coupling between superconducting grains or to stronger flux pinning of the intergranular vortices induced by the presence of silver. The combined effect of both these factors may also be responsible for this improvement. This paper presents a study of the flux dynamics in YBCO/Ag composites under low and high fields by measurements of M–H loop and AC susceptibility. Analysis of

both inter- and intragranular contributions to magnetization has been carried out. The determination of the critical fields is limited by the granular nature of these materials, wherein the magnetic field enters the intergranular regions before it penetrates into the superconducting grains. So there exist two kinds of lower and upper critical fields corresponding to the intergrain (H_{c1j} and H_{c2j}) and intragranular (H_{c1g} and H_{c2g}) regions. Hence a perfect field screening state in the granular superconductor exists for fields lower than H_{c1j}. This value of H_{c1j} may serve as a measure of the strength of the intergrain coupling in these materials.

The measurement of the lower critical field H_{c1} is based on any one of the following criteria defining the first field for flux penetration: (i) deviation from the Meissner state (Aguillon and Senoussi 1990) (onset of nonlinearity in M vs H curve), (ii) onset of irreversibility above the critical field (Yeshurun *et al* 1988), and (iii) field-dependent penetration depth in high-quality crystal (Sridth *et al* 1989). We have used the second method of the onset of irreversibility in this study.

2. Experimental

To prepare the YBCO/Ag composites the solid-state reaction method was employed. The calcined YBCO powder mixed with silver powder (0–20 wt%) was pressed into pellets and sintered at 950°C for 15 h in flowing oxygen. These samples were characterized for electrical resistivity, transport J_c and microstructure. The DC magnetization measurements at 77 K as a function of field were carried out using a vibrating sample magnetometer (VSM) (model DMS 1660). DC magnetization data were recorded for YBCO/Ag composites in sintered compact form. The samples had a rectangular bar shape with dimensions nearly 14 mm × 2·5 mm × 2 mm. Measurements were carried out in zero field cooled (ZFC) state with maximum field (H_{max}) of 200 mT (expressed as $\mu_0 H$). Also, the AC susceptibility measurements at an AC frequency of 3970 Hz at different AC fields (0·026–0·30 mT) were carried out in the temperature range 77–100 K. Transport J_c (with 1 μV/cm criterion) measurements were carried out at 77 K under zero magnetic field.

3. Results and discussion

The scanning electron microscope was used to study the grain morphology of the YBCO/Ag composites. The pure sample exhibited a broad distribution of grain sizes with an average grain size of 5–6 μm. Addition of silver resulted in uniform grain size distribution with enhanced grain growth and better intergrain connectivity. The grain growth was maximum around 15% silver content (average grain size ≈ 25 μm). The microstructural details with silver content are given in table 1. Electrical resistivity measurements show that all these samples had a transition temperature around 92 K. Transport J_c measurements have shown a two-fold increase in J_c for an Ag content up to 10% compared to the pure sample (table 1).

Figure 1 shows the M–H curves of pure YBCO and YBCO/Ag composites under low fields (up to $H_{max} = 4$ mT). In figure 1a (pure sample), the variation of M with H is nearly linear and slightly irreversible when the maximum applied field in an M–H cycle, H_{max}, is 0·5 mT. Therefore for this sample Josephson lower critical field $H_{c1j} < 0{\cdot}5$ mT. Also, for YBCO/Ag composites a small hysteresis can be seen at 0·5 mT

Table 1. Grain size and transport critical current density of YBCO/Ag composites.

% Silver	Grain size (μm)	Transport J_c (A/m^2 × 10^4)
0	6	185
5	15	250
10	15	350
15	25	200
20	20	80

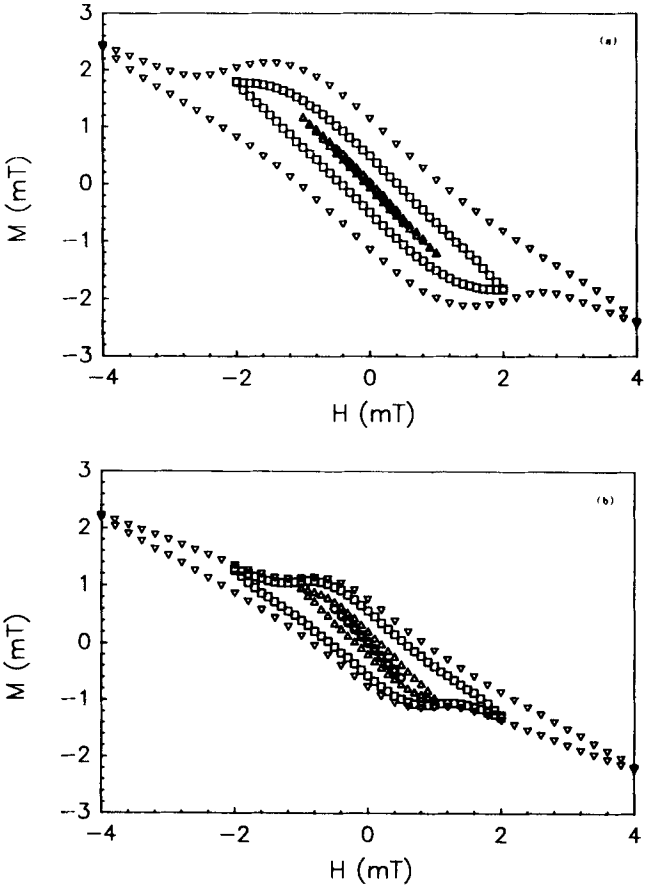

Figure 1. M–H curves of YBCO/Ag composites up to $H_{max} = 4$ mT: (a) 0% Ag, (b) 5% Ag.

(figure 1b). This shows that for all these pure YBCO and YBCO/Ag composites H_{c1j} is less than 0·5 mT. H_{c1j} is a complicated function of intergranular critical current density and grain size (Tinkham and Lobb 1989) and is given by

$$H_{c1j} = (2\pi a J_{cj}/c)\ln(3\Phi_0 c/32 J_{cj} a^3)^{1/2}, \tag{1}$$

where a is the grain size and J_{cj} the intergrain critical current density. As we have seen from microstructural studies the grain size increases with addition of silver. Also

the transport measurements show increase in J_{cj} up to 10% Ag. The combined effect of both the factors increases H_{c1j} slightly, but this could not be observed at the lower limit of our set-up (i.e. 0·5 mT). For $H < H_{c1j}$, the diamagnetism is associated with the persistent macroscopic currents circulating around the sample. When the applied field exceeds H_{c1j}, hysteresis arises due to the pinning of the intergranular vortices. In this state, both intergranular and London currents (around grains) coexist in the sample. With increase in H_{max}, the curve becomes reversible but with a reduced slope. The hysteresis curve is made up of a reversible linear portion above a certain field superimposed on the irreversible region centred around the origin. Similar behaviour has been observed in sintered specimens of the other families of HTSCs (Senoussi *et al* 1987; Grover *et al* 1988). This second field, where reversibility sets in and the intergranular currents vanish, corresponds to H_{c2j} (Senoussi *et al* 1987). By comparing the M–H plots of YBCO/Ag composites, it can be seen that with increasing silver content H_{c2j} decreases. This can be explained on the basis of the effect of grain size. According to Tinkham and Lobb, H_{c2j} depends only on the grain size and is inversely proportional to the square of the grain size, and is given by

$$H_{c2j} = 3\pi\Phi_0/8a^2. \tag{2}$$

H_{c2j} varies from 2·8 mT to 1·0 mT when silver content varies from 0 to 20 wt% (figure 2). This decreasing trend is in qualitative agreement with Tinkham and Lobb.

In figure 1, it can be clearly seen that the width of hysteresis depends upon the value of H_{max} for that loop. Senoussi *et al* (1987) have shown that the critical state concept (Kim *et al* 1963; Bean 1964) was only partially suitable to describe the low-field magnetic behaviour of superconducting ceramics. According to Bean's model, for a homogeneous slab of thickness d with field applied in the slab plane, the equation for magnetization can be written as

$$\Delta M = H_{max}^2/2H^* \quad \text{for} \quad H_{max} < H^*$$

and

$$\Delta M = H^*/2 \quad \text{for} \quad H_{max} > H^*,$$

where H^* is the full penetration field given by $J_c d/2$. These can be written as

$$\Delta M d \propto H_{max}^2/J_c \quad \text{for} \quad H_{max} < H^*$$

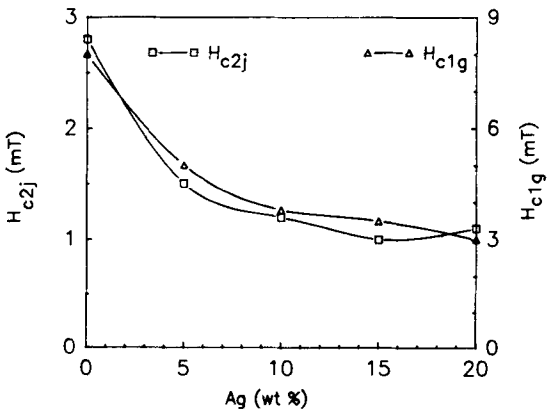

Figure 2. H_{c2j} and H_{c1g} vs silver content.

and

$$\Delta M/d \propto J_c \qquad \text{for} \quad H_{max} > H^*.$$

It can be seen very clearly that for $H < H^*$, ΔM is a function of H_{max} and inversely proportional to J_c, whereas it is directly proportional to J_c and independent of H_{max} for $H > H^*$.

The intergrain critical current density from magnetization J_{cjm} can be written as

$$J_{cjm}(\text{A/cm}^2) = 20(M^- - M^+)/d = 20\,\Delta M/d \quad \text{for} \quad H_{max} > H^*, \tag{3}$$

where $\Delta M = (M^- - M^+)$, H^* is the full penetration field, and M^- and M^+ are the magnetizations (in emu/cm^3) in the decreasing and increasing directions of the fields respectively.

The full penetration field H^* can be determined by the overlap of the M–H loops with increasing H_{max} (Calzona *et al* 1989). If we compare the M–H curve of YBCO/Ag composites for $H > H^*$ (figure 3a) following Bean's formalism, at any value of field YBCO/Ag composites have lower $\Delta M/d$ ($\sim J_c$) compared to the pure YBCO sample. But the curves at $H_{max} < H^*$ show a different kind of behaviour (figures 3b and c). These figures reveal that up to a certain silver content the width of hysteresis is higher for YBCO/Ag composites depending upon H_{max}. This behaviour can be seen from the variation of $|\Delta M|_{H=0} \cdot d$ for different H_{max} (figure 4). This variation has been shown for different silver concentrations. For any composition, $\Delta M \cdot d$ starts to show saturation at relatively higher fields. YBCO/Ag composites have higher $\Delta M \cdot d$ compared to the pure sample up to a certain field. This shows that J_{cjm}'s of YBCO/Ag composites are lower compared to the pure sample. The use of Bean's model to extract information about J_c from low-field M–H loop of HTSCs is not correct as the model assumes J_c to be independent of field. Further it assumes that $H_{c1} = 0$. These granular superconductors show a strong field dependence of transport J_c. The low-field M–H loops are superimposed on the reversible contribution of grain magnetization. The grain size (D_g) also affects the width of hysteresis (Maury *et al* 1990). Increase in grain size decreases the width of low-field hysteresis. Furthermore decrease in intragranular critical current density increases the ΔM of low-field M–H loop. The contribution of grains also increases with decrease in H_{c1g}. This low-field behaviour is a complicated function of field dependence of J_{cj}, grain size and intragranular critical current density. With silver content, grain size is increasing and intragrain current is decreasing. So ΔM is a combined effect of D_g and J_{cgm}. Therefore, estimation of J_{cjm} for the intergranular region from low-field data is very difficult (Calzona *et al* 1989; Goldfarb *et al* 1993).

As the field exceeds H_{c2j}, the grains get decoupled and the magnetization is governed mainly by the London currents circulating around the grains. This linear and reversible behaviour of M–H continues till H_{max} becomes greater than a third critical field H_{c1g}, which marks the onset of field penetration inside the grains. In the pure YBCO sample, it can be clearly seen that this reversible behaviour continues up to 8 mT (figure 5), but with silver addition the value of H_{c1g} decreases and lies around 5 and 3·8 mT for 5 and 10% Ag contents respectively (figure 2). H_{c1g} depends upon the intragranular critical current density of the sample. When H_{max} exceeds H_{c1g}, the M–H loop takes on a new z-type shape (figure 6). The magnetization goes through a maximum and then decreases monotonically with H. This behaviour is governed by intragrain vortices and is similar to the M–H loop of conventional type-II

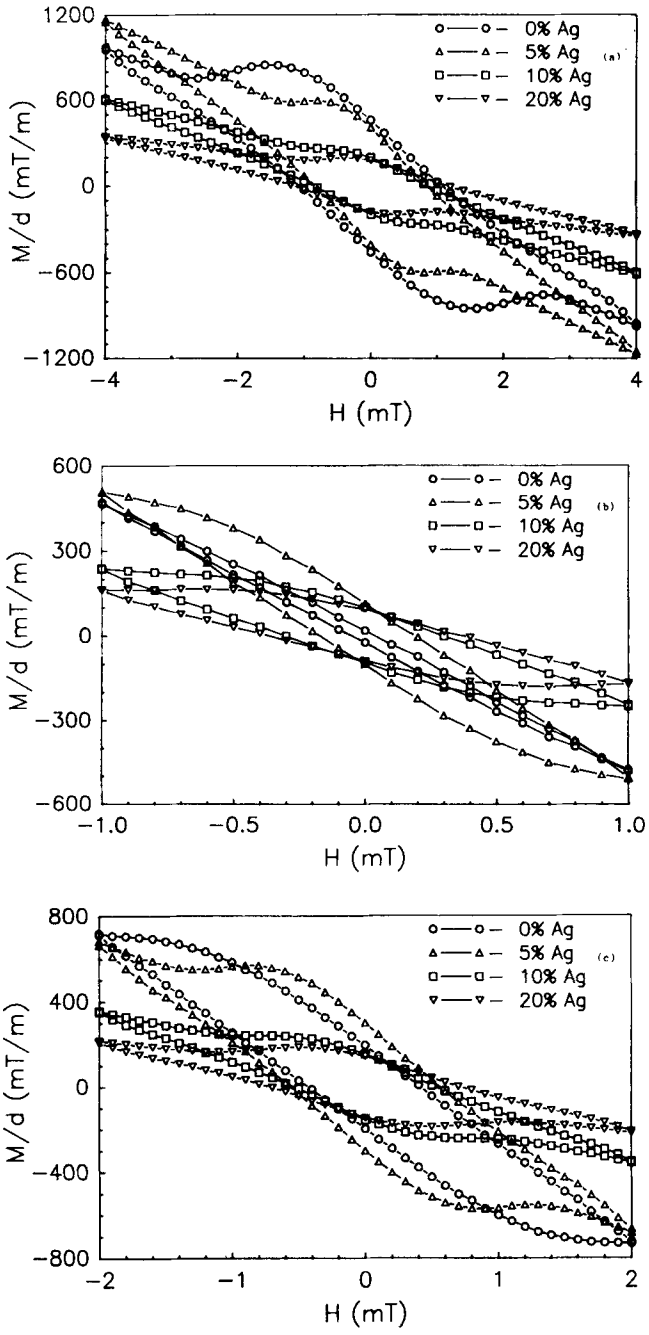

Figure 3. M–H curves for different silver contents at different H_{max}: (a) $H_{max} = 4$ mT, (b) $H_{max} = 1$ mT and (c) $H_{max} = 2$ mT.

superconductors. In figure 6, it can be seen that the addition of Ag made the curve less hysteretic compared to the pure one. The magnitude of the hysteresis, ΔM, in the M–H curve is determined by that of the shielding current induced inside the grains. Intragrain critical current density has been calculated with the help of (3),

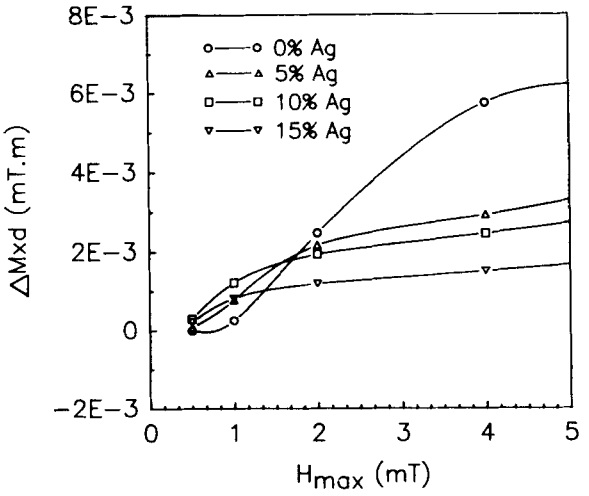

Figure 4. $\Delta M \cdot d$ vs H_{max} for different silver contents.

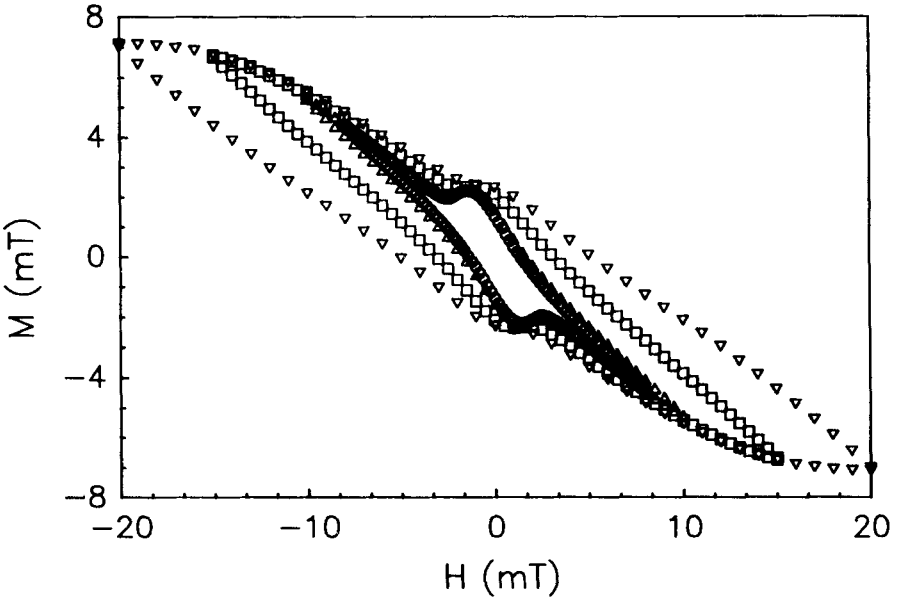

Figure 5. M–H curve for 0% Ag at $H_{max} = 8$, 10, 15 and 20 mT.

only replacing d by the grain size. It can be inferred that the intragrain J_{cgm} shows a maximum at non-zero field. This anomalous feature of increase in J_{cgm} with field has been observed by others also but still cannot be explained (Tholence 1988; Xu *et al* 1989). J_{cgm} decreases with silver addition and the value lies in the range 10^9–10^8 amp/m^2 (figure 7). The results of Ag addition at higher fields are in agreement with the other reports (Jung *et al* 1990; Xia *et al* 1993). This decrease in intragrain critical current density is responsible for the decrease in H_{c1g} with Ag content.

AC susceptibility measurements have also been used for calculation of $J_{cj}(T)$ from the peak of the imaginary component. The slope of the J_{cj} vs temperature curve

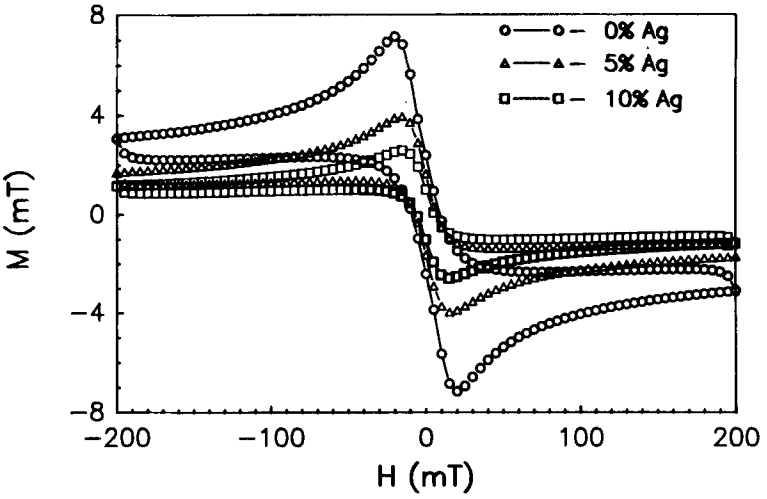

Figure 6. M–H curve at $H_{max} = 200$ mT for different Ag contents.

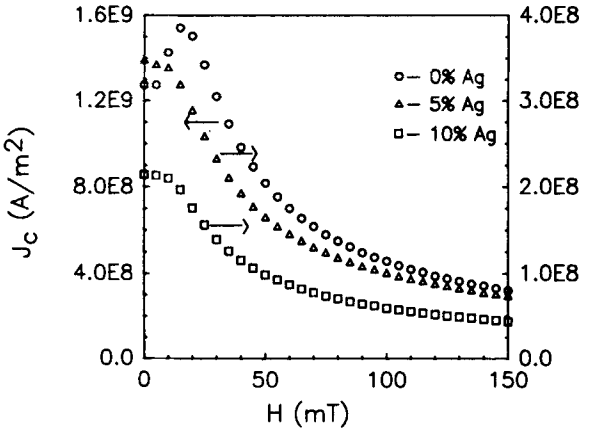

Figure 7. Intragrain J_{cgm} vs H for different Ag contents.

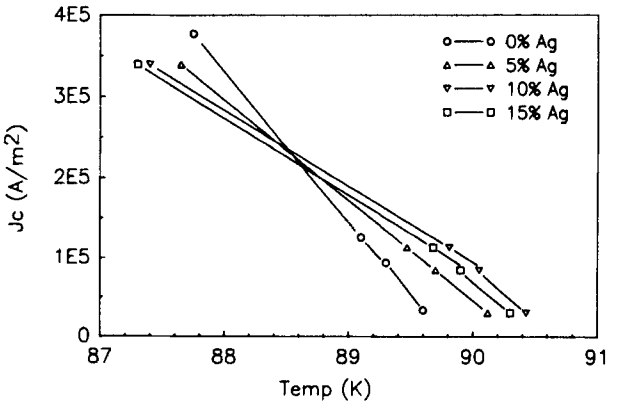

Figure 8. Intergrain J_{cj} vs T from susceptibility for various Ag contents.

(figure 8) decreases with increasing Ag concentration, indicating thereby that addition of Ag changes the coupling between the grains. At higher temperatures (or low AC fields) J_c increases with silver content and is maximum at 10% Ag content, beyond which it decreases, and vice versa at lower temperatures (or high AC fields). These results at very low values of AC fields are in agreement with the transport measurements of J_c under zero field. This AC susceptibility is not sensitive to the reversible contribution of magnetization from the grains. This improvement in J_{cj} can be explained on the basis of decrease of the junction resistance. According to Ambegaokar and Baratoff (1963), when the intergranular junctions are Josephson weak links, the critical current is given by

$$I_c = (\pi/eR_n)\Delta(T)\tanh(\Delta(T)/2k_B T),$$

where $\Delta(T)$ is the temperature-dependent energy gap parameter and R_n the junction's normal-state tunneling resistance. As R decreases with the addition of silver, the junction resistance R_n is expected to be lowered, resulting in a higher shielding current. The critical current variation is given by

$$I_c \propto (1 - T/T_c)^{3/2}.$$

But if the links are S–N–S junction, then

$$I_c = (1 - T/T_c)^2 \exp(-2d_n/\zeta),$$

where d_n is the thickness of the normal metal layer and ζ is the coherence length. When this coupling changes at higher silver content due to increase in d_n, I_c decreases.

4. Conclusions

Comparison of the magnetization data on YBCO/Ag composites reveals that H_{c2j} and H_{c1g} decrease with increasing addition of silver. The low-field M–H loop shows complicated behaviour as the silver content varies. The effect of grain size, intragrain critical current density (J_{cgm}) and decrease of H_{c1g} makes the low-field M–H loop very complicated. Determination of intergranular critical current density J_{cjm} from this low-field loop is not a simple function of ΔM. The high-field M–H loop corresponding to the intragrain region (≈ 200 mT) also shows a decrease in magnetic J_{cgm} with increasing silver content. However, the AC susceptibility and transport measurements show improvement in J_{cj} with increasing silver content. This shows that addition of silver improves intergrain J_{cj} up to a certain point only due to the improvement in intergrain coupling but does not help in pinning. In fact, it degrades the intragrain J_{cgm} values.

Acknowledgements

The authors gratefully acknowledge DNPL and CSIR for providing the funds and infrastructural facilities to carry out this work. The authors thank Sandip Dhara for his assistance in M–H loop measurements. One of the authors (ID) also acknowledges the fellowship provided by DST.

References

Aguillon C and Senoussi S 1990 *J. Less Common Metals* **164–165** 1061
Ambegaokar V and Baratoff A 1963 *Phys. Rev.* **B10** 486
Baliga S and Jain A L 1989 *Appl. Phys.* **A49** 139
Bean C P 1964 *Rev. Mod. Phys.* **36** 31
Calzona V, Cimberle M R, Ferdeghini C R, Putti M and Siri A S 1989 *Physica* **C157** 425
Dhingra I, Padam G K, Singh S, Tripathi R B, Rao S U M, Suri D K, Nagpal K C and Das B K 1991 *J. Appl. Phys.* **70** 1775
Dwir B, Affronte M and Pavuna D 1989 *Appl. Phys. Lett.* **55** 399
Goldfarb R B, Cross R W, Goodrich L F and Bergen N F 1993 *Cryogenics* **33** 3
Grover A K, Radhakrishnamurthy C, Chaddah P, Ravi Kumar G and Subba Rao G V 1988 *Pramana – J. Phys.* **30** 569
Jung J, Mohamed M A K, Cheng S C and Franck J P 1990 *Phys. Rev.* **B42** 6161
Kim Y B, Hempstead C F and Strand A R 1963 *Phys. Rev.* **129** 528
Matsumoto Y, Hombo J, Yamaguchi Y and Nishida M 1990 *Appl. Phys. Lett.* **56** 1585
Maury R, Fert A R, Redoules J P, Ayache J, Sabras J and Monty C 1990 *Physica* **C167** 591
Pavuna D, Berger H, Affronte M, Maas J Van Der, Caponi J J, Guillot M, Lejay P and Tholence J L 1988 *Solid State Commun.* **68** 535
Ren Y, Meng J, Niu M and Zeng Z 1990 *Solid State Commun.* **76** 1103
Saito Y, Noji T, Endo A and Higuchi N 1987 *Jpn. J. Appl. Phys.* **26** L832
Sen S, Chen I G, Chen C H and Stefanescu D M 1989 *Appl. Phys. Lett.* **54** 766
Senoussi S, Ousenna M and Ribault M 1987 *Phys. Rev.* **B36** 4003
Singh J P, Leu H L, Poeppel R B, Voorhees E Van, Goudey G T, Winsley K and Shi D 1989 *J. Appl. Phys.* **66** 3154
Sridth S, Wu Dong Ho and Kennedy W 1989 *Phys. Rev. Lett.* **63** 1873
Tholence J L 1988 *Physica* **C153–155** 1479
Tiefel T H, Jin S, Sherwood R C, Davis M E, Kammlott G W, Gallagher P K, Johnson D W, Fastenacht Jr R A and Rhodes W W 1988 *Mater. Lett.* **6** 555
Tinkham M and Lobb C J 1989 *Solid State Phys.* **42** 91
Xia J A, Ren H T, Zhao Y, Andrikidis C, Liu H K and Dou S K 1993 *Supercond. Sci. Tech.* **6** 315
Xu Y, Guan W, Zeibig K and Heiden C 1989 *Cryogenics* **29** 281
Yeshurun Y, Malozemoff A P, Holtzberg F and Dinger T R 1988 *Phys. Rev.* **B38** 11828